Research article

Didang Tang inhibits intracerebral hemorrhage-induced neuronal injury via ASK1/MKK7/JNK signaling pathway, network pharmacology-based analyses combined with experimental validation

Jing Lu [a,b], Xiaolei Tang [a], Dongmei Zhang [c], Tianye Lan [d], Qingxia Huang [a], Peng Xu [d], Miao Liu [b], Li Liu [e,**], Jian Wang [d,*]

[a] Research Center of Traditional Chinese Medicine, The Affiliated Hospital to Changchun University of Chinese Medicine, Jilin, China
[b] College of Traditional Chinese Medicine, Changchun University of Chinese Medicine, Jilin, China
[c] Research Office, The Affiliated Hospital to Changchun University of Chinese Medicine, Jilin, China
[d] Department of Encephalopathy, The Affiliated Hospital to Changchun University of Chinese Medicine, Jilin, China
[e] College of Pharmacy, Changchun University of Chinese Medicine, Jilin, China

ARTICLE INFO

ABSTRACT

Background: Intracerebral hemorrhage (ICH) is an acute cerebrovascular disease, which is also a principal consideration for disability. Didang tang (DDT) is a classic traditional Chinese medicine formula for treating ICH. However, its pharmacological mechanism of action has not been elucidated.

Materials and methods: The TCMSP and BATMAN-TCM databases were used to collect chemical compounds and predict targets of DDT. Protein targets in ICH were identified by GeneCards, OMIM, and DrugBank databases. DDT compounds-ICH targets and protein-protein interaction (PPI) networks were constructed for topological analysis and hub-targets screening. Further, Key biological processes and signaling pathways were identified by GO and KEGG enrichment analyses. Then, an ICH rat model and a Cobaltous Chloride (CoCl$_2$)-induced PC12 cells model were established. Cell viability and lactate dehydrogenase (LDH) release were detected using cck8 and LDH kits. Apoptosis levels were detected by TUNEL assessment and flow cytometry. IL-1β levels were detected by ELISA, while key protein expressions were determined by Western blot.

Results: A total of 126 active compounds related to DDT and 3,263 therapeutic targets for ICH were predicted. The functional enrichment of the GO and KEGG pathways combined with literature studies suggested that DDT is most likely to influence MAPK and apoptotic signaling pathways for ICH treatment. In vitro and in vivo experiments have shown that DDT remarkably inhibited apoptosis and increased the expression of Bcl-2, while inhibiting Bax and cleaved-Caspase 3. For other enriched core proteins, DDT suppressed the phosphorylation of Src and the expression of c-Myc and IL-1β, and up-regulated the level of MMP-9. The further results showed that, DDT decreased the phosphorylation of ASK1, MKK7, JNK and c-JUN.

Conclusion: Based on network pharmacology and experimental validation results, our *in vivo* and *in vitro* study indicated that ASK1/MKK7/JNK pathway might be the critical target for DDT against ICH.

1. Introduction

Intracerebral hemorrhage (ICH) accounts for 12–20% of the world's stroke incidence. ICH has extremely serious consequences, with mortality rate of up to 40% in the acute phase, and 60%–80% of survivors have severe neurological damage, which ranks first in acute cerebrovascular disease [1]. Although the advance in minimally invasive endoscopic intracerebral hemorrhage evacuation has reduced mortality, the prognosis of ICH is still unsatisfactory [2]. Therefore, scholars have turned their attention to reducing the secondary brain injury induced by ICH, which has crucial preclinical significance.

Neuronal apoptosis is widely considered as one of the primary mechanisms for secondary nerve injury and neurological deficit after ICH [3]. Inhibition of neuronal apoptosis may be a promising therapeutic

---

* Corresponding author.
** Corresponding author.
E-mail addresses: 13596199046@163.com (L. Liu), jian-w222@163.com (J. Wang).

strategy for the treatment of ICH. It is generally regarded that the MAPK pathway is closely related to regulating neuronal apoptosis [4]. MAPK signaling, which directs cellular responses to various stimuli, acts as the essential pathway in regulating cell proliferation and differentiation, stress response and apoptosis [5]. Studies have shown that apoptosis signal-regulated kinase 1 (ASK1) was ubiquitinated and phosphorylated to play an active role after ICH [6]. Activated ASK1 can promote the mitogen-activated protein kinase kinase (MAPKK) 7 phosphorylate, which further activates Thr and Tyr residues of MKK7 to phosphorylate JNK [7, 8]. A subset of activated JNKs directly regulate the activities of apoptotic-related mitochondrial proteins. Another part transactivates pro-apoptotic genes, including c-JUN, through specific transcription factors [9].

The advantages of traditional Chinese medicine (TCM) in the treatment of ICH have gradually become prominent [10, 11]. In Chinese medicine, the pathological core of acute cerebral hemorrhage was recorded as blood stasis [12, 13]. Didang Tang (DDT) is composed of leeches (chinese name: Shuizhi, Latin name: *Hirudo nipponica* Whitman), gadflies (chinese name: Mengchong, Latin name: *Tabanus bivittatus* Mats.), peach seeds (chinese name: Taoren, Latin name: *Prunus persica*(L.) Batsch) and rhubarbs (chinese name: Dahuang, Latin name: *Rheum palmatum* L.), which sources from *Treatise on Febrile Disease*. The initial treatment of DDT was for severe blood accumulation, which is currently extensively used to treat ICH [14, 15]. Clinical studies demonstrated that DDT has outstanding effects in improving the clinical symptoms of ICH patients, reducing the extent of neurological deficits, and promoting absorption of hematomas [16, 17]. Neuroprotective effects of DDT were also observed in rats with ICH, findings showed that DDT could increase nerve growth factor expression, and inhibit neuronal apoptosis induced by endoplasmic reticulum stress [18, 19]. Moreover, DDT can improve hypoxia-induced neuronal endoplasmic reticulum stress, and inhibiting aluminum chloride-induced neuronal oxidative damage [20, 21]. Peach seeds, one of the components of DDT, inhibit BV-2 microglial activation induced by LPS [22]. As a neuroprotective agent, emodin improves antioxidant capacity and mitochondrial function in a variety of disorders affecting the nervous system [23, 24, 25]. Hirudin exert neuroprotective effects on patients who have sustained acute cerebral infarctions by regulating serum matrix metalloproteinase 9 [26]. Thus, DDT was conjectured to have a protective effect on neuronal apoptosis after cerebral hemorrhage. However, its mechanism of action remains unclear.

Network pharmacology is a subject based on biological systems to discover the synergistic effect and potential mechanism of drug multi-targets [27]. In this work, we utilized network pharmacology to analyze the possible activities and molecular mechanisms of DDT to alleviate ICH-induced CNS damage.

2. Materials and methods

2.1. Preparation of DDT and high-performance liquid chromatography (HPLC) analysis

Herbal Slices in DDT were supplied by the Affiliated Hospital of Changchun University of Traditional Chinese Medicine. As previously described, DDT was extracted from 4 Chinese herbals (Table 1) [20]. Briefly, using 10 times volume of water to soak the mixed compound for 30 min, and then extract it at 100 °C for 30 min for 3 times, and combine

the extracts. Brownish powder is obtained by centrifuging, filtering and freezing the supernatant. Quality control of DDT was analyzed by HPLC. The mobile phase consists of 0.1% acetic acid in water (A), and acetonitrile-water (B). The column temperature was 25 °C, and the flow rate was 0.9 mL/min, with UV detection at 254 nm. Analyzing retention time was conducted using Gallic acid, Amygdalin, Sennoside B, Rhein-8-O-β-D-glucopyranoside, Sennoside A, Aloeemodin, Rhein, Emodin and Physcion as the control (Figure 1A). We observed 9 peaks of DDT based on retention time comparisons with standards (Figure 1B). Following that, HPLC fingerprints of DDT were analyzed with Chinese Medicine Chromatographic Fingerprint Similarity Evaluation System (2012 Edition). For all 10 batches analyzed, the similarities were greater than 0.98 overall, suggesting that our DDT has good reproducibility overall (Figure 1C).

2.2. DDT chemical composition collection and target screening

Network pharmacology analysis was completed according to standard procedures recommended by Li's team [28]. Chemical compositions of DDT were searched using TCMSP (http://tcmspw.com/tcmsp.php) and Bioinformatics Analysis Tool for Molecular mechANism of TCM (BATMAN-TCM, http://bionet.ncpsb.org/batman-tcm/) database. The filter criteria for the chemical composition of DDT were oral bioavailability (OB) ≥30% and drug-likeness (DL) ≥0.18. Unobtained target components were supplemented with the help of the Swiss TargetPrediction database (http://www.swisstargetprediction.ch/). Finally, the "component-target gene" network was visualized by the UniProt database (https://www.uniprot.org/) and Cytoscape 3.8.2 software.

2.3. ICH targets screening

The targets of ICH were obtained using GeneCards (https://www.genecards.org/), OMIM (https://www.ncbi.nlm.nih.gov/omim) and DrugBank (https://go.drugbank.com/) database.

2.4. Active ingredients-targets network

We Used Weishengxin online platform (http://www.bioinformatics.com.cn) to obtain a Venn diagram that representing "DDT active components-ICH disease targets". Moreover, Cityscape 3.8.2 software was used for later visualization and further topology analysis.

2.5. Protein-protein interaction (PPI) network

Protein interactions was obtained by the String database (https://string-db.org/), which took Medium confidence>0.4 as the screening condition. CytoNCA and string App plugin were provided support for visualization.

2.6. Pathway enrichment analyses

Gene ontology (GO) and Kyoto Encyclopedia of Genes and Genomes (KEGG) enrichment analysis of common target genes were fulfilled by the omicshare platform (https://www.omicshare.com/), g:Profiler platform (http://biit.cs.ut.ee/gprofiler/gost), and R language analysis. The

Table 1. Components of the DDT.

| Chinese name	English name	Latin name	Family	Plant part(s)	Proportion	Voucher specimen
Da huang	Rhubarb	*Rheum palmatum* L.	Polygonaceae	Root and rhizome	1	202109–23
Tao ren	Peach seed	*Prunus persica*(L.) Batsch	Rosaceae	Seed	3	202109–24
Meng chong	Gadfly	*Tabanus bivittatus* Mats., *Tabanus mandarinus* Schiner	Tabanidae	Whole body	1	202109–25
Shui zhi	Leech	*Hirudo nipponica* Whitman, *Whitmania pigra* Whitman, *Whitmania acranulata* Whitman	Hirudunidae	Whole body	1	202109–26
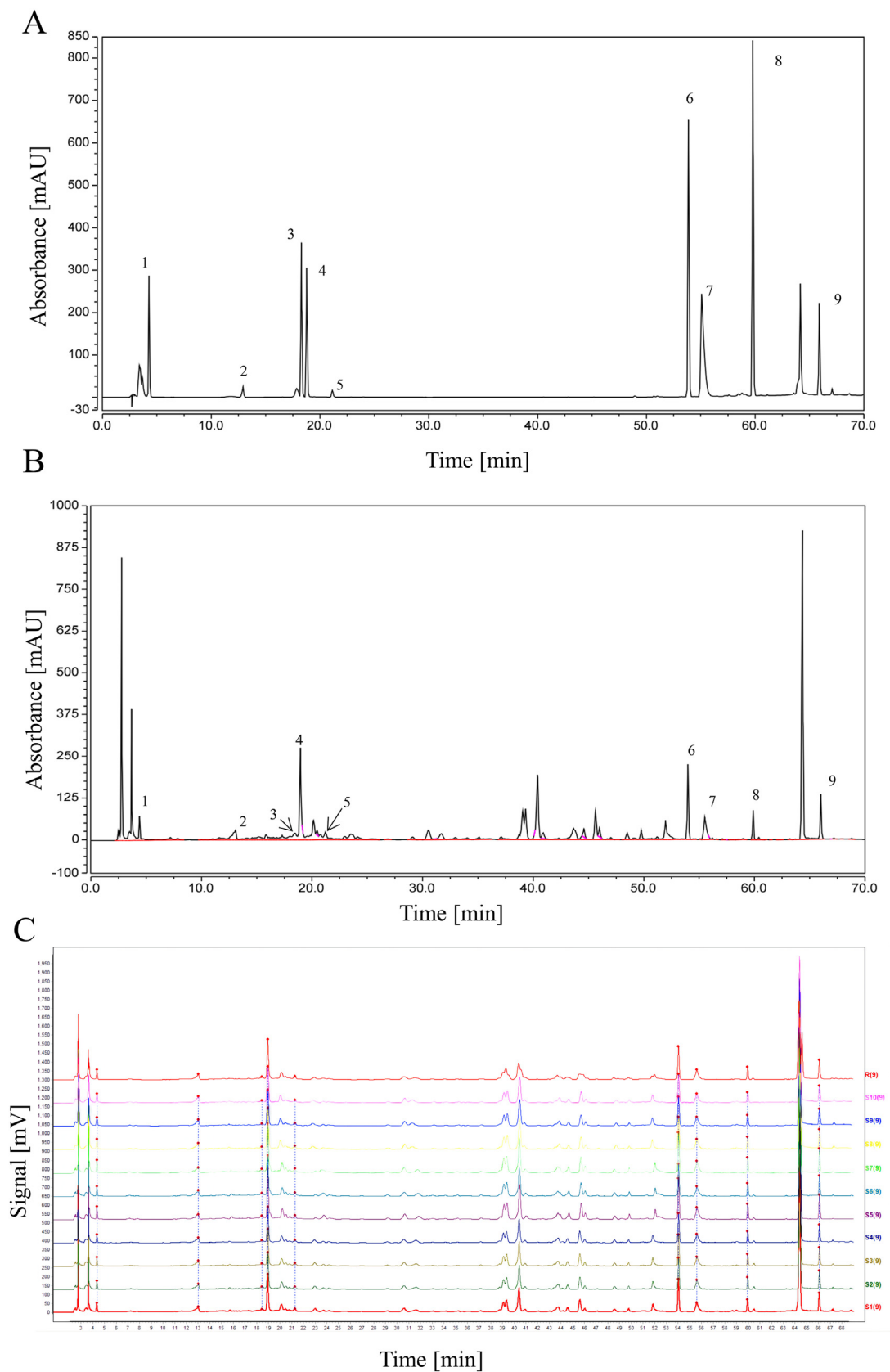
Figure 1. High-Performance Liquid Chromatography (HPLC) Analysis of DDT. (A) HPLC chromatograms of mixed standards with UV detection conducted at 254 nm. 1: Gallic acid, 2: Amygdalin, 3: Sennoside B, 4: Rhein-8-O-β-D-glucopyranoside, 5: Sennoside A, 6: Aloeemodin, 7: Rhein, 8: Emodin, 9: Physcion. (B) HPLC chromatogram of DDT. (C) HPLC fingerprints for 10 batches of DDT.

enrichment process took p ≤ 0.05, and species were choosing as as "*Homo sapiens*" as the filter conditions.

2.7. ICH modeling

The research was conducted in accordance with the internationally accepted principles for laboratory animal use and care in the European Community guidelines (EEC Directive of 1986; 86/609/EEC), and was approved by the Experimental Animal Committee of Changchun University of Traditional Chinese Medicine (NO. 2021125). Rats, provided by the Animal Center of Jilin University, were randomly split into sham group, ICH group and ICH + different doses of DDT group (1.3 g/kg, 2.6 g/kg, 5.2 g/kg). For DDT group, intragastric administration was started 2 h after ICH, twice a day for a total of 5 days. Models for ICH were established as described previously [29]. Briefly, rats were placed in a stereotaxic frame after being anesthetized with isoflurane. A hole was drilled three millimeters right and four millimeter posterior of the bregma, and 50μl of 0.9% sterile saline or autologous blood were injected into the skull at a depth of 6.5 m with a 26-gauge needle in 5 min. The wound was sutured and the hole sealed with bone wax. Throughout the procedure, the body temperature was maintained at 37 °C, and after waking up, the rats had free access to food and water.

2.8. Tunel assay

Brain tissues were sectioned and stained with tunel assay according to the instructions. Tunel-positive cells was photographed and calculated at 400× magnification in 5 randomly selected microscope fields [30].

2.9. IL-1β measurement by ELISA

Brain tissues from untreated and DDT-treated rats or culture supernatant from PC12 cells were collected and the level of IL-1β was determined using ELISA kits, according to the manufacturer's instructions [31].

2.10. Western blot analysis

The lysed protein was, detected by BCA kit. Then, we used 10 % or 12 % SDS- PAGE to separate proteins (40 μg). After transferthem to the PVDF membranes, they were blocked with 5 % BSA, and incubated with specific primary antibodies (p- Src, Src, Cl-Caspase3, c-JUN, p-c-JUN, p-ASK1, ASK1, p-MKK7, MKK7, Bcl-2, Bax, MMP-9, c-Myc, p-JNK, JNK, GAPDH, 1:1,000) overnight at 4 °C. PVDF membranes were incubated with 1:5000 secondary antibodies (1:5,000) for 1 h at room temperature in the next day. Finally, we applied a chemiluminescent imaging software (ProteinSimple, CA, USA) to visualize the protein bands and further quantitative analysis [32].

2.11. Cell viability

The PC12 cell line was cultured within the RPMI-1640 medium with 5% FBS and 10% horse serum at 37 °C with 5% CO2. To build a hypoxia injury model, 3×10^3 cells were plated to each well of a 96-well plate and continuous culture in differentiation medium, which containing 50 ng/mL nerve growth factor (NGF), for 72 h. Different concentrations of Cobaltous Chloride (CoCl2) were added into each well for 24 h. Cells treated with CoCl2 were incubated with different concentrations of DDT (25, 50 and 100 μg/mL) and examined with CCK8 [33].

2.12. Lactate dehydrogenase (LDH) activity

We used an LDH assay kit to measure the activity of LDH. Culture mediums were collected and measured according to the manufacturer's introduction [34].

2.13. Flow cytometry analysis

Apoptosis of PC12 cells treatment with DDT and/or CoCl2 was analyzed using Annexin V-FITC/PI kit. Briefly, cells (4×10^5) was first incubated with 6 μL FITC for 15 min, and then stained with 5 μL PI for another 5 min. After washing with PBS, we used flow cytometry to determine apoptotic rate [35].

2.14. Statistical analysis

Data were expressed as the mean ± standard deviation. GraphPad Prism software was conducted to examine all statistical analyses. One-way ANOVA test (Turkey's *post hoc*) was used to examine statistical significance. $p < 0.05$ was considered significant in statistics.

3. Results

3.1. Interaction networks of DDT active compounds and ICH therapeutic targets

Altogether, 126 active compounds related to DDT were obtained from the published literature (Table 2). Further, we obtained 234 targets corresponding of DDT through searching the TCMSP and BATMAN-TCM database. Meanwhile, 3,263 disease targets for ICH were collected from the OMIM, DrugBank and GeneCards databases. Through comparing the targets of DDT and ICH, 124 common matched targets were acquired by VENNY analysis (Figure 2A). With the help of Cytoscape, an interaction network was built to find out the intrinsic relationships between corresponding compounds of DDT and ICH (Figure 2B), which contained 231 nodes and 581 edges.

3.2. PPI network construction

The core gene network of the intersection genes was constructed using the STRING database and Cytoscape 3.8.2 software. CytoNCA plugin was used for the first screening, and the thresholds were: CC > 0.44、EC > 0.04、BC > 62.02、LAC > 11.34、DC > 26.00、NC > 13.58. According to the degree value, the top 35 key targets were screened and listed as hub genes for DDT treatment in ICH (Figure 3A). Then, using the string App plugin, set the Confidence (score) cutoff to 0.4 to draw a network of key protein interactions. Combined with the literature and the pathological process of ICH, 6 key core verification nodes were finally screened (Figure 3B). Meanwhile, DDT showed a strong regulation of IL-1β, JUN, SRC, CASP3, MMP9 and Myc, which involved apoptosis. Targets with more than 40 neighboring nodes were listed, among which IL-1β protein scored the highest for its connection with 110 adjacent nodes (Figure 3C).

3.3. GO and KEGG enrichment analyses

We performed GO and KEGG analysis on 124 intersecting genes to obtain enriched functional clusters. For GO enrichment analysis, we obtained 6,580 GO items. Among these items, BP, CC and MF accounted for 80.84%, 7.8% and 11.32%, respectively. Moreover, the proportions of p < 0.05 in these three parts were 59.73%, 51.55% and 60%, separately (Figure 4A). Further, we depicted the top 20 GO items of BP, CC and MF. Results demonstrated that targets of DDT for ICH in BP mainly participated in positive regulation of the nutrient levels and metal ion. In the aspect of CC, the targets primarily occurred in the synaptic membrane, mitochondrial matrix, and neuron spine. Obviously, the MF was mainly associated with participating in DNA binding transcription factor binding, nuclear receptor activity and neurotransmitter receptor activity (Figure 4B).

For KEGG enrichment analysis, we got 157 KEGG items. The OmicShare platform and the pathview package in the R language software were utilized to visualize pathway diagram of DDT in the treatment of ICH. The pathway annotation diagram in Figure 4C showed that, amino acid metabolism, cell growth and death, nervous system and

Table 2. The active ingredients of DDT.

MOLnumber	MOLname
MOL012955	3beta-cholesta-5,24-dien-3-ol
MOL012254	Campesterol
MOL009679	Delta(sup 7)-Cholestenol
MOL005449	L-Methionine, homopolymer
MOL005448	L-Leucine, homopolymer
MOL005402	Methyl Heptadecanoat
MOL003969	L-Serine, homopolymer
MOL002321	Proline, 5-oxo-, L-
MOL002302	Rhapontin
MOL002301	DLA
MOL002300	10beta-Hydroxy-6beta-isobutyrylfuranoeremophilane
MOL002299	DMR
MOL002297	Daucosterol_qt
MOL002295	Cinnamic acid
MOL002288	Emodin-1-O-beta-D-glucopyranoside
MOL002286	Laccaic acid D
MOL002285	1-O-Galloyl-glycerol
MOL002284	PIT
MOL002283	[(2R,3S,4S,5R,6S)-6-[4-[(Z)-2-(3,5-dihydroxyphenyl)ethenyl]phenoxy]-3,4,5-trihydroxyoxan-2-yl]methyl 3,4,5-trihydroxybenzoate
MOL002281	Toralactone
MOL002280	Torachrysone-8-O-beta-D-(6′-oxayl)-glucoside
MOL002279	Serotonin
MOL002267	Rhein diglucoside
MOL002268	3-O-p-coumaroylquinic acid
MOL002262	5-[(Z)-2-(3-hydroxy-4-methoxy-phenyl)vinyl]resorcinol
MOL002261	ZINC04081604
MOL002259	Physciondiglucoside
MOL002258	Physcion-9-O-beta-D-glucopyranoside_qt
MOL002256	1,8-dihydroxy-3-methoxy-2,6-dimethyl-9,10-anthraquinone
MOL002249	Gallocatechin
MOL002247	Emodin-6-glucoside
MOL002244	Chrysophanol glucoside
MOL002243	Anthraglycoside B
MOL002240	5-Carboxy-7-hydroxy-2-methyl-benzopyran-gamma-one
MOL002238	3-Hydroxy-25-norfriedel-3,1(10)-dien-2-one-30-oic acid
MOL002235	Eupatin
MOL002231	(−)-Epicatechin-pentaacetate
MOL002230	(+)-Catechin-pentaacetate
MOL001986	β-sitosterol
MOL001880	OXL
MOL001794	MAE
MOL001780	L-Tryptophane
MOL001744	Uracil
MOL001732	Glycerol
MOL001729	Crysophanol
MOL001456	Citric acid
MOL001369	Grandidentatin
MOL001368	3-O-p-coumaroylquinic acid
MOL001366	MNN
MOL001363	GA97
MOL001362	GA95
MOL001361	GA87
MOL001360	GA77
MOL001359	GA70
MOL001358	Gibberellin 7
MOL001355	GA63
MOL001353	GA60
MOL001352	GA54

Table 2 (*continued*)

MOLnumber	MOLname
MOL001351	Gibberellin A44
MOL001349	4a-formyl-7alpha-hydroxy-1-methyl-8-methylidene-4aalpha,4bbeta-gibbane-1alpha,10beta-dicarboxylic acid
MOL001347	GA16
MOL001345	Methyl-alpha-D-fructofuranoside
MOL001344	GA122-isolactone
MOLX	Hirudin
MOL001342	GA121-isolactone
MOL001340	GA120
MOL001338	GA118
MOL001335	WLN: Q1R
MOL001333	7-dehydroavenasterol
MOL001332	RMN
MOL001331	Amygdalinic acid
MOL001330	2,3-didehydro GA9
MOL001329	2,3-didehydro GA77
MOL001328	2,3-didehydro GA70
MOL001327	2,3-didehydro GA69
MOL001323	Sitosterol alpha1
MOL001321	D-mandelonitrile
MOL001320	Amygdalin
MOL001316	Campesterol-3-O-β-D-glucopyranoside_qt
MOL001315	Campesterol-3-O-β-D-glucopyranoside
MOL001301	Cis-Zimtsaeure
MOL001237	O-Acetyltoluene
MOL000953	Cholesterol
MOL000666	Hexanal
MOL000513	3,4,5-trihydroxybenzoic acid
MOL000493	Campesterol
MOL000476	Physcion
MOL000472	Emodin
MOL000471	Aloe-emodin
MOL000421	Nicotinic acid
MOL000397	Cis-p-Coumarate
MOL000358	Beta-sitosterol
MOL000346	Succinic acid
MOL000296	Hederagenin
MOL000295	Alexandrin
MOL000131	EIC
MOL000096	(−)-catechin
MOL000071	L-Histidine, homopolymer
MOL000069	Palmitic acid
MOL000068	Isoleucine
MOL000067	(S)-Valine
MOL000065	L-aspartic acid
MOL000059	Uridine, labeled with tritium
MOL000054	L-Arginine, homopolymer
MOL000052	L-Glutamic acid, homopolymer (9CI)
MOL000050	Glycine
MOL000041	Phenylalanine (VAN)

neurodegenerative diseases were highly enriched pathways related to DDT for ICH. Results demonstrated that the MAPK signaling pathway (has:04010) and the apoptosis signaling pathway (has:04210) were closely related to the treatment of ICH with DDT (Figure 4D and E).

3.4. DDT relieves nerve damage of ICH

In the light of the network pharmacology results, we speculated that DDT mainly exerted its protective effect by inhibiting neuronal apoptosis. Moreover, IL-1β also played an essential role in PPI analysis. Based on
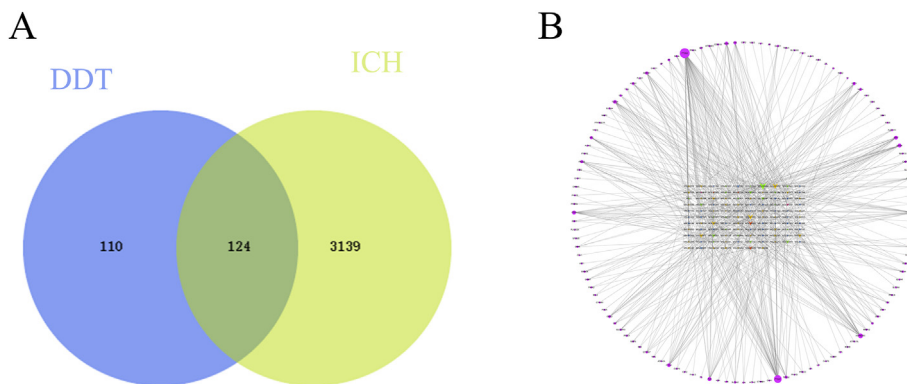
Figure 2. The construction of DDT-target-ICH. (A) Venn diagram describing targets distribution of DDT and ICH. (B) DDT-target-ICH network. The outer circle represents target proteins associated with ICH, and the inner circle refers to DDT active ingredients.
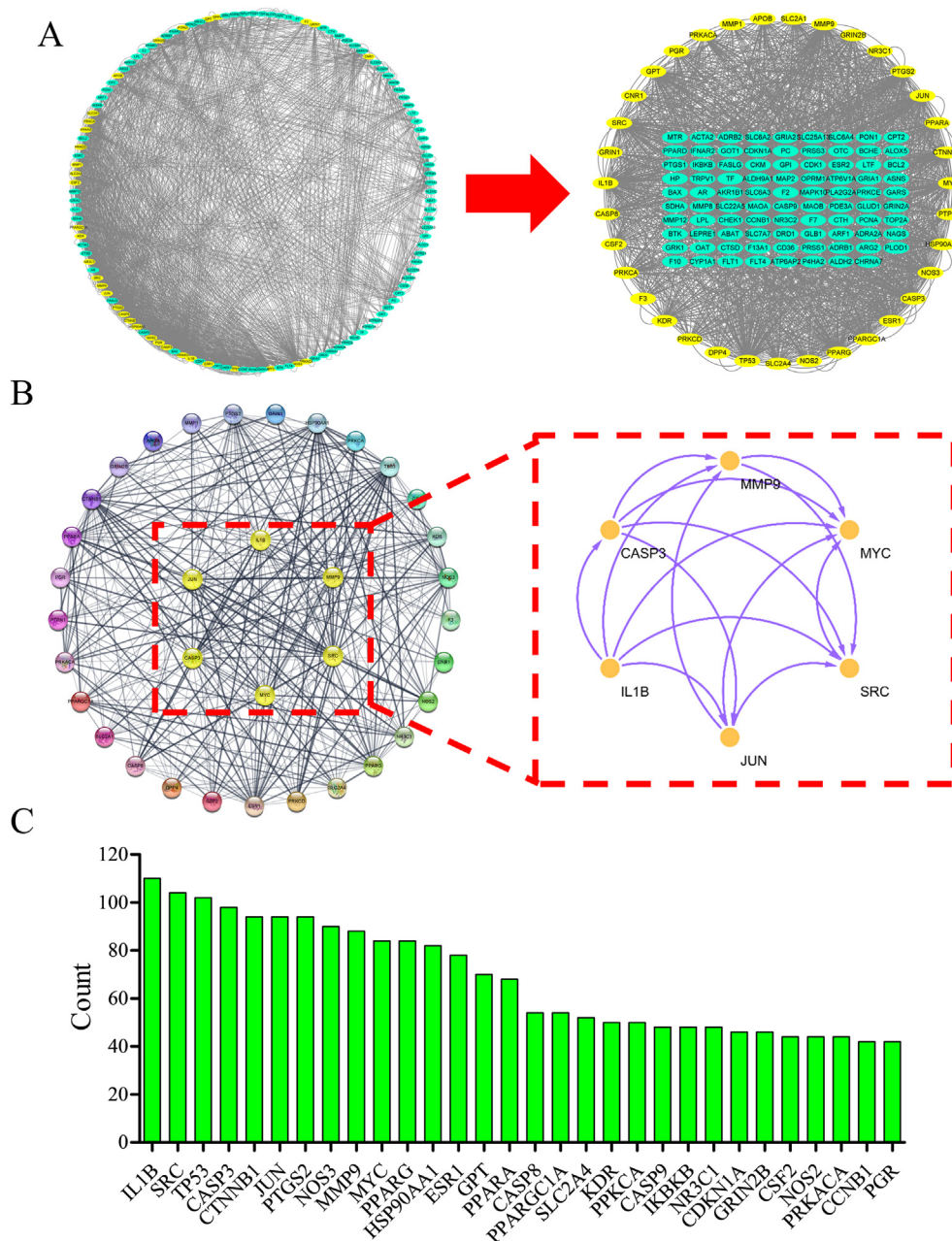

Figure 3. Protein-protein interaction (PPI) network of DDT target for the treatment of ICH. (A) Hub genes of DDT for ICH. The top 35 key targets were screened by degree value using the CytoNCA plugin. (B) STRING analysis of the PPI network of DDT targets for treating ICH. Different colored spheres represent target genes, with protein structures inside. Lines indicate interactions between protein targets. The thicker lines represent the more considerable degree of the target node. (C) Statistical analysis of (B) The X-axis represented the name of the protein, and the Y-axis represented the number of network neighbor nodes.
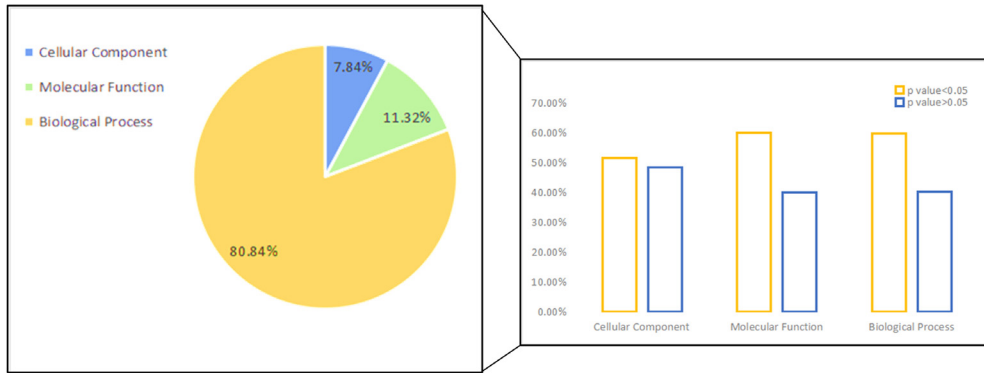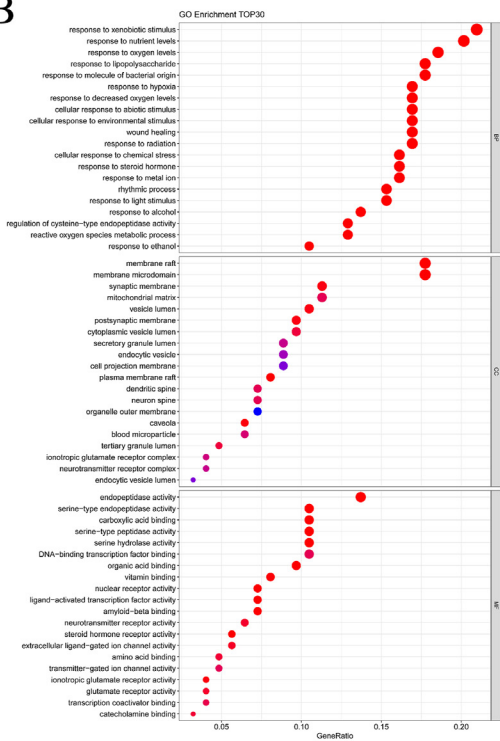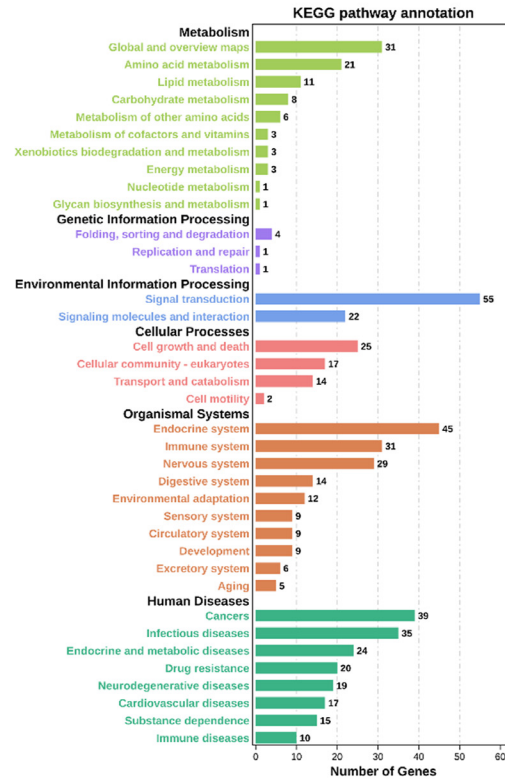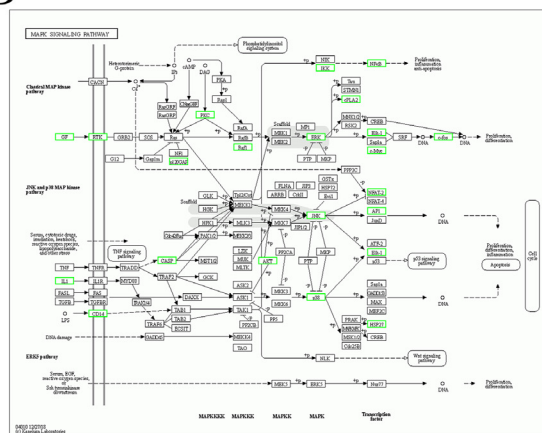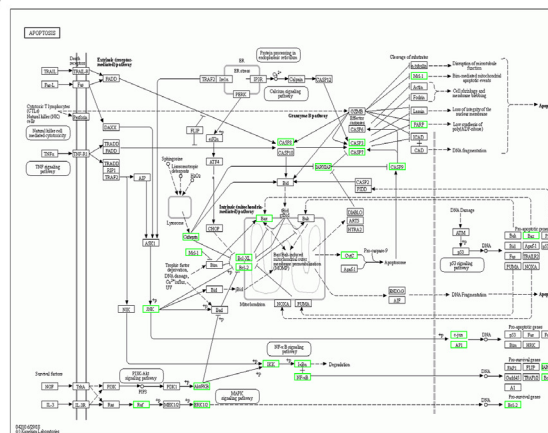
Figure 4. GO and KEGG Enrichment Analyses. (A) Three types of GO gene and gene product attributes in the database were shown (blue, cellular component; green, molecular function; yellow, biological process). (B) GO annotation analysis for the top 20 targets. (C) KEGG annotation analysis for the top 20 targets. (D) The most correlated signaling pathway related to DDT treatment of ICH in KEGG mapper - MAPK signaling pathway (has:04010) and apoptosis signaling pathway (has:04210).

these results, we established a rat model of ICH, in which the anti-apoptotic and anti-inflammatory effects of DDT were evaluated by tunel staining and Elisa analysis (Figure 5A). Figure 5B and C illustrated that in contrast to the ICH group, 2.6 g/kg and 5.2 g/kg of DDT treatment markedly inhibited the number of tunel positive cells. Elisa assay indicated that 1.3 g/kg, 2.6 g/kg and 5.2 g/kg of DDT suppressed the level of IL-1β (Figure 5D). We demonstrated that DDT could significantly relieve nerve damage caused by ICH.

3.5. DDT reduces neuronal apoptosis via ASK1/MKK7/JNK signaling pathway in rats

To further confirm the beneficial impact of DDT in ICH rats, we validated the key proteins obtained by hub gene analysis combined with

PPI analysis. The previous results found that the HD group had the best therapeutic effect on ICH, so this group was selected for futher experimental verification. Western blot results indicated that DDT suppressed Src phosphorylation and the expression of c-Myc and IL-1β (Figure 6A). Moreover, DDT up-regulated the expression of MMP-9 to 2.19 fold (Figure 6A).

Previous results suggested that DDT might exert protective effects by inhibiting apoptosis. As expected, our Western blot results demonstrated that Bcl-2 with an anti-apoptotic effect showed an increasing trend with DDT treatment. However, Bax and cleaved-Caspase 3 with pro-apoptotic impact fell back to average level (Figure 6B).

Moreover, based on KEGG and PPI analysis, we speculated that the JNK signaling pathway might be a critical pathway for DDT to regulate apoptosis. In our study, DDT decreased the phosphorylation of ASK1,
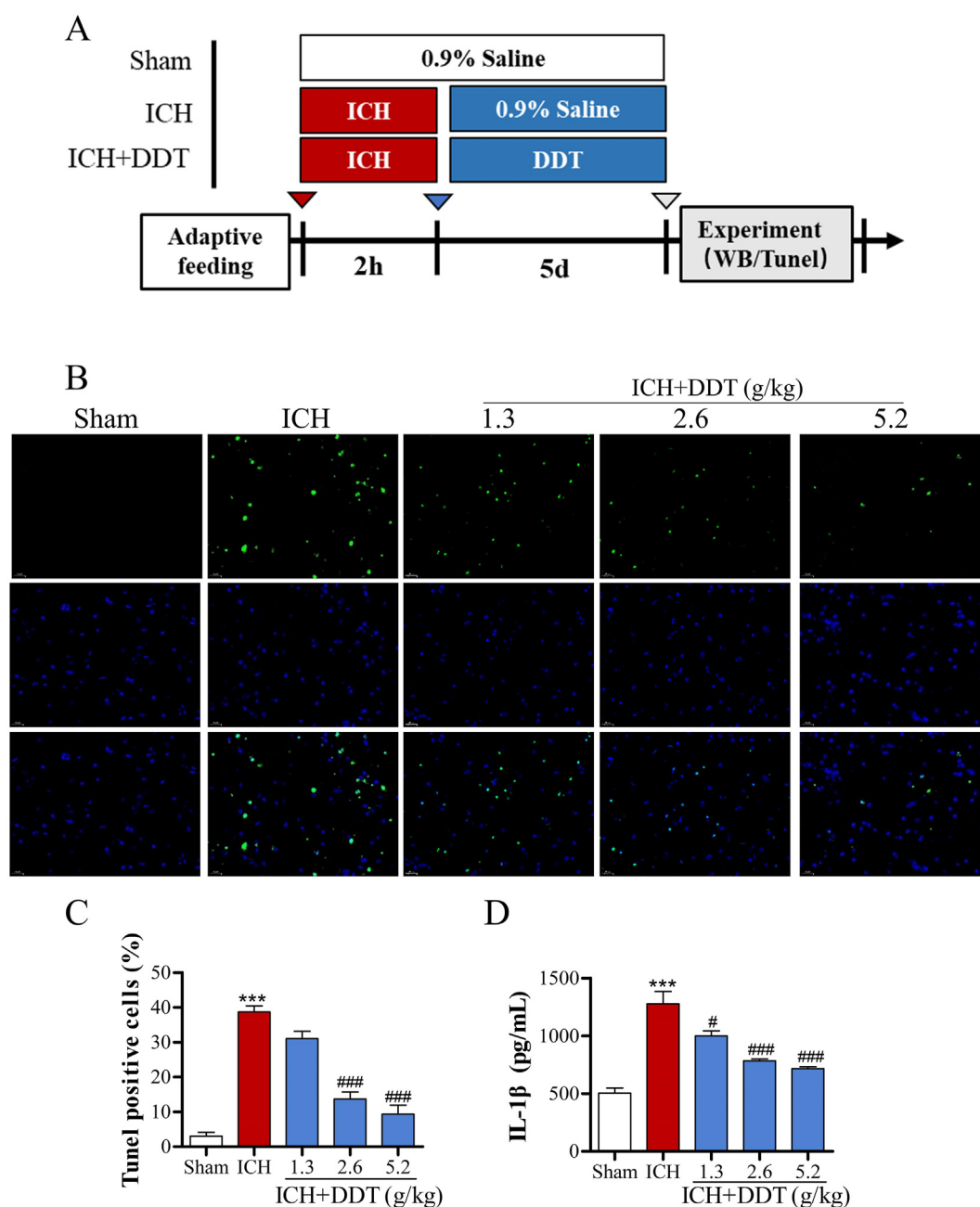

Figure 5. DDT relieves nerve damage of ICH. (A) Diagram of the animal study for the ICH model or the DDT treatment groups. (B) Representative images of tunel staining of brain tissues (n = 5, Original magnification ×400). (C) Statistical analysis of tunel staining was shown. (D) IL-1β level was measured by Elisa kit. ***$p < 0.001$ vs. sham group; #$p < 0.05$, ###$p < 0.001$ vs. ICH model group.
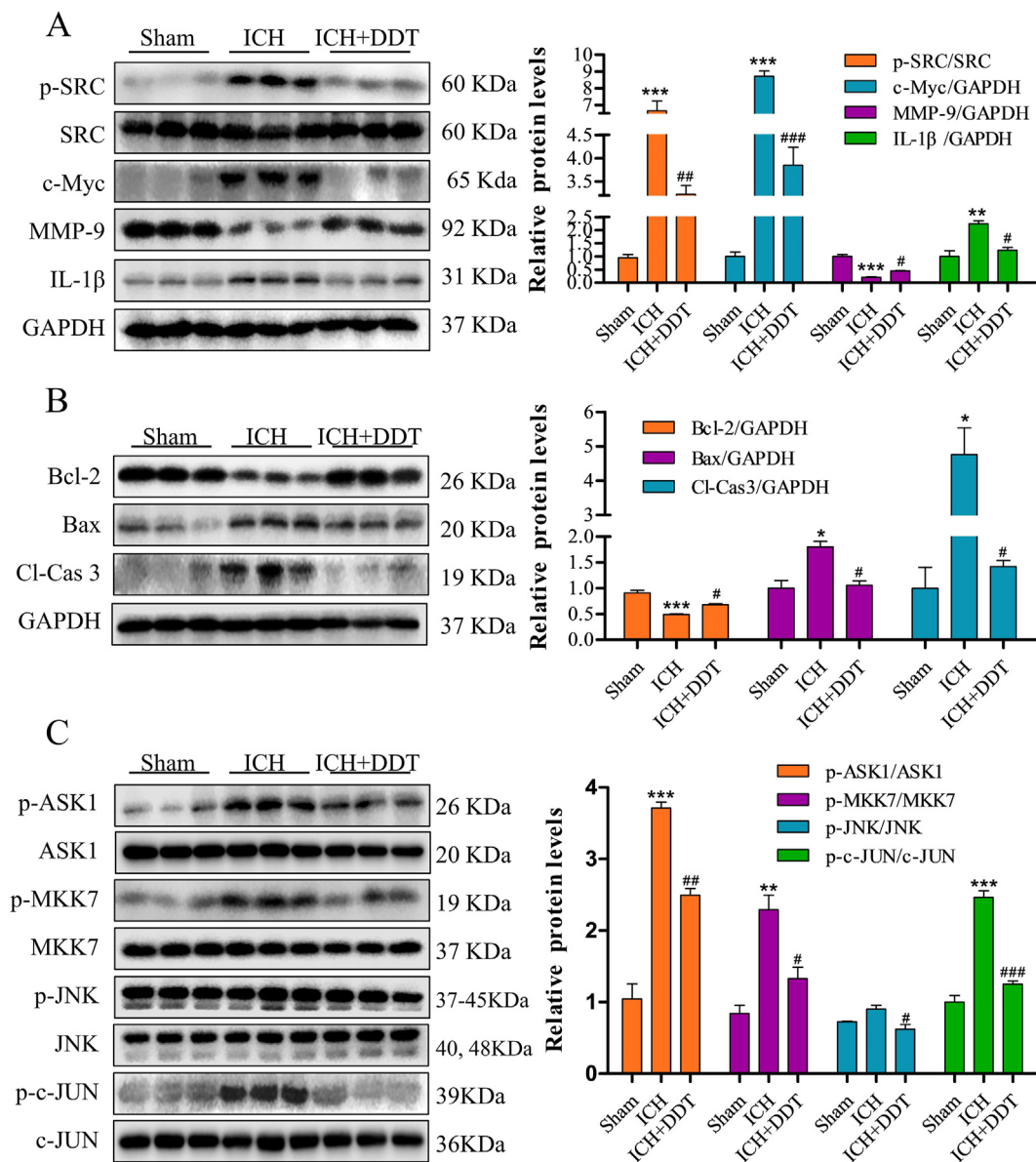
Figure 6. DDT reduces neuronal apoptosis via ASK1/MKK7/JNK signaling pathway in rats. (A) Western Blotting analysis of p-Src (Sup F. 1), Src (Sup F. 2), c-Myc (Sup F. 3), MMP-9 (Sup F. 4) and IL-1β (Sup F. 5). On the basis of normalization to GAPDH (Sup F. 6), the relative expression levels of each protein were calculated and is shown on the right. (B) The expression of apoptotic related proteins Bcl-2 (Sup F. 7), Bax (Sup F. 8) and cleaved-Caspase 3 (Sup F. 9) by western blotting, with quantitative analysis on the right (using GAPDH (Sup F. 10) as a control). (C) The expression of JNK signaling related proteins p-ASK1 (Sup F. 11), ASK1 (Sup F. 12), p-MKK7 (Sup F. 13), MKK7 (Sup F. 14), p-JNK (Sup F. 15), JNK (Sup F. 16), p-c-JUN (Sup F. 17), c-JUN (Sup F. 18) by Western blot analysis. Quantitative analysis of the protein production levels was shown on the right. $*p < 0.05$, $**p < 0.01$, $***p < 0.001$ vs. sham group; $^{#}p < 0.05$, $^{##}p < 0.01$, $^{###}p < 0.001$ vs. ICH model group.

MKK7, JNK and c-JUN (Figure 6C). We demonstrated that DDT significantly inhibited apoptosis via ASK1/MKK7/JNK signaling pathway.

3.6. DDT increased the cell viability and inhibited IL-1β release in CoCl₂-induced PC12 cells

To further confirm the protective impact of DDT on neurons, we established a CoCl₂-induced hypoxic injury model of PC12 cells. Results showed that CoCl₂ at the concentration from 31.25 to 1000 μg/mL reduced cell viability and promoted IL-1β release in a dose-dependent response (Figure 7A, B). And we choose 200 μg/mL as the modeling condition for further experiments. Results showed that DDT can restore the cell viability and alleviate IL-1β level induced by CoCl₂ in PC12 cells (Figure 7C, D).

3.7. DDT protected against CoCl₂-induced PC12 cells apoptosis

In order to study beneficial impact of DDT on CoCl₂-induced PC12 cells, we firstly verified the key proteins enriched before. As shown in Figure 6A, in contrast to the CoCl₂ group, DDT treatment markedly restrained the phosphorylation of Src and the expression of c-Myc and IL-1β (Figure 8A, B). Meanwhile, DDT significantly increased the expression of MMP-9 (Figure 8A, B).

In addition, we conducted a further study on the anti-apoptotic effect of DDT. After simulation of CoCl₂, the apoptosis rate increased to 25.83% in contrast to control group, but normalized when treated with DDT (Figure 8C, D). Moreover, DDT increased the expression of Bcl-2 and decreased Bax and cleaved-Caspase 3 expression, respectively (Figure 8E, F). Therefore, we confirmed that DDT could restrain the apoptosis of PC12 cells induced by CoCl₂.
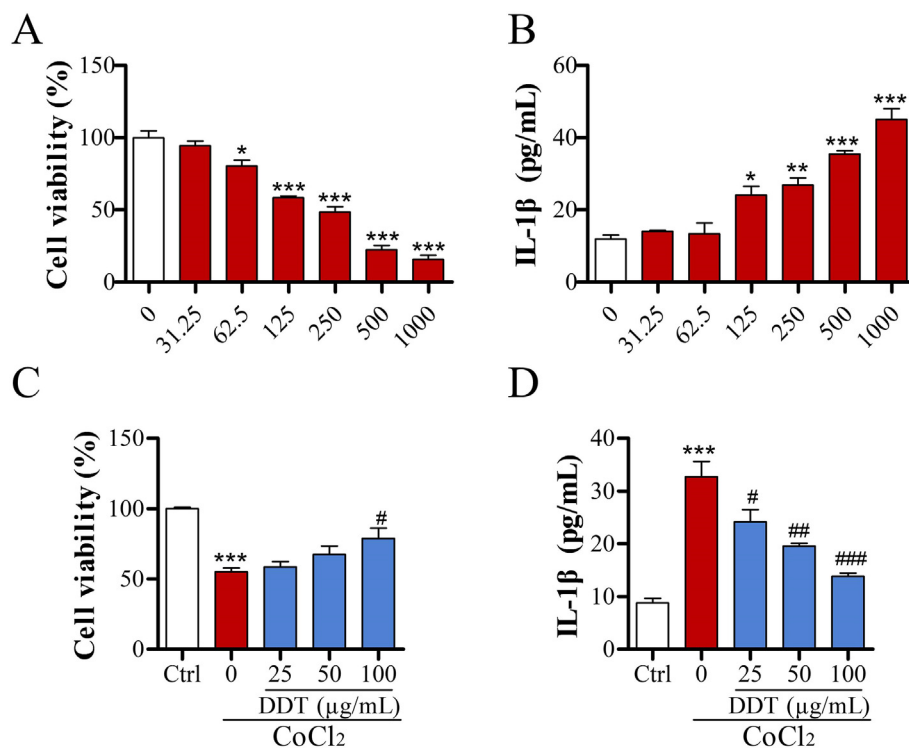
3.8. DDT ameliorated CoCl$_2$-induced PC12 cells apoptosis via ASK1/MKK7/JNK signaling pathway

We further investigated the related proteins of JNK signaling. Results displayed that CoCl$_2$ facilitated the phosphorylation of ASK1, MKK7, JNK and c-JUN visibly, which were decreased by treatment of DDT (Figure 9A, B). Moreover, we selected SP600125, a JNK-specific inhibitor, to probe whether the JNK signaling pathway mediated the key role of DDT in CoCl$_2$-induced apoptosis. We found that incubation with SP600125 suppressed the DDT effect on CoCl$_2$-induced p-JNK, Bax and cleaved-Caspase 3 (Figure 9C, D). These consequences revealed that DDT protected PC12 cells from CoCl$_2$-induced apoptosis by regulating the ASK1/MKK7/JNK signaling pathway.

4. Discussion

DDT is a classic prescription for the treatment of ICH. Network pharmacology is an effective method to discover the relationship between drugs, targets and diseases [27]. Modern research mainly uses it to build multicomponent-multitarget-multipathway networks and predict the mechanism of TCM in various illnesses. In this research, we used Network pharmacology to find that the mechanism of DDT in the treatment of ICH is related to apoptosis mediated by the MAPK pathway. Furthermore, we used ICH rat modeling and CoCl$_2$-induced PC12 cells model to verify the antiapoptosis activity of DDT. Results showed that DDT inhibits neuronal apoptosis after ICH by regulating ASK1/MKK7/JNK signaling pathway. These results laid a strong foundation upon which to build further research to reveal the mechanism of DDT.

On the basis of the number of nodes in the "DDT-target-ICH" network, 35 hub genes were screened. By further combining the relationship between key proteins and the pathological process of cerebral hemorrhage, we finally screened six key cores, which are IL-1β, JUN, SRC, CASP3, MMP-9 and c-Myc, respectively. Studies have shown that MMP-9 and CASP3 are directly involved in apoptosis after ICH [36]. Furthermore, c-Myc and c-JUN participated in regulating neuronal apoptosis through dimerization, respectively [37, 38]. Src, as a proto-oncogene, is one of the non-receptor protein tyrosine kinase family [39]. As an inflammatory factor, IL-1β can also promote apoptosis by promoting an inflammatory response [40]. Meanwhile, GO and KEGG enrichment analyses indicated that apoptosis was the essential part in the biological processes and signaling pathways. Therefore, we determined the beneficial impact of DDT on neuronal apoptosis in the ICH rats model and the CoCl$_2$-induced PC12 cells model. As expected, DDT inhibited the calculation of apoptotic cells (Figure 5B, C and Figure 8C). For the key proteins enriched, DDT treatment markedly inhibited the phosphorylation of Src and the expression of c-Myc and IL-1β. Meanwhile, DDT significantly increased the expression of MMP-9 (Figure 6A and Figure 8A, B). Furthermore, DDT increased the expression of Bcl-2 and decreased cleaved-Caspase 3 and Bax expression, respectively (Figure 6B and Figure 8E, F). Thus, the consequences demonstrated that DDT could remarkably restrain nerve cell apoptosis and improve nerve cell damage after intracerebral hemorrhage.

KEGG pathway analysis showed that the MAPK signaling pathway was significantly enriched. MAPKs regulate numerous biological processes, especially cell proliferation and death in response to external stimuli. Besides, MAPKs activate signaling cascades upon phosphorylation, which induce conformational changes in MAPKs that ultimately lead to enhanced catalytic activity [41, 42]. Our finding indicated that the phosphorylation levels of ASK1, MKK7 and JNK were increased after ICH injury (Figure 6C and Figure 9A, B). Studies have shown that various apoptosis stimulators can activate ASK1 and phosphorylate MKK7, ultimately resulting in JNK activation, which induces apoptosis. In addition, phosphorylated JNK is transported to the nucleus by an oblique pathway, where c-JUN is activated by phosphorylation to induce further apoptosis [43, 44, 45]. According to our PPI analysis, c-JUN is one of the key targets for DDT to exert protective effects (Figure 3B, C). Therefore, we speculate that DDT can inhibit the ASK1/MKK7/JNK signaling pathway and activate c-JUN through an indirect pathway, thereby inhibiting neuronal apoptosis. Indeed, our results confirmed this inference, treatment with DDT significantly reduced the phosphorylation of ASK1, JNK, MKK7 and c-JUN (Figure 6C and Figure 9A, B). JNK inhibitor, SP600125, was also applied to validate our results. Results showed that the addition of SP600125 further improved DDT-induced suppression of p-JNK, Bax and Cl-Casp3 levels (Figure 9C). Our findings suggest that DDT treatment
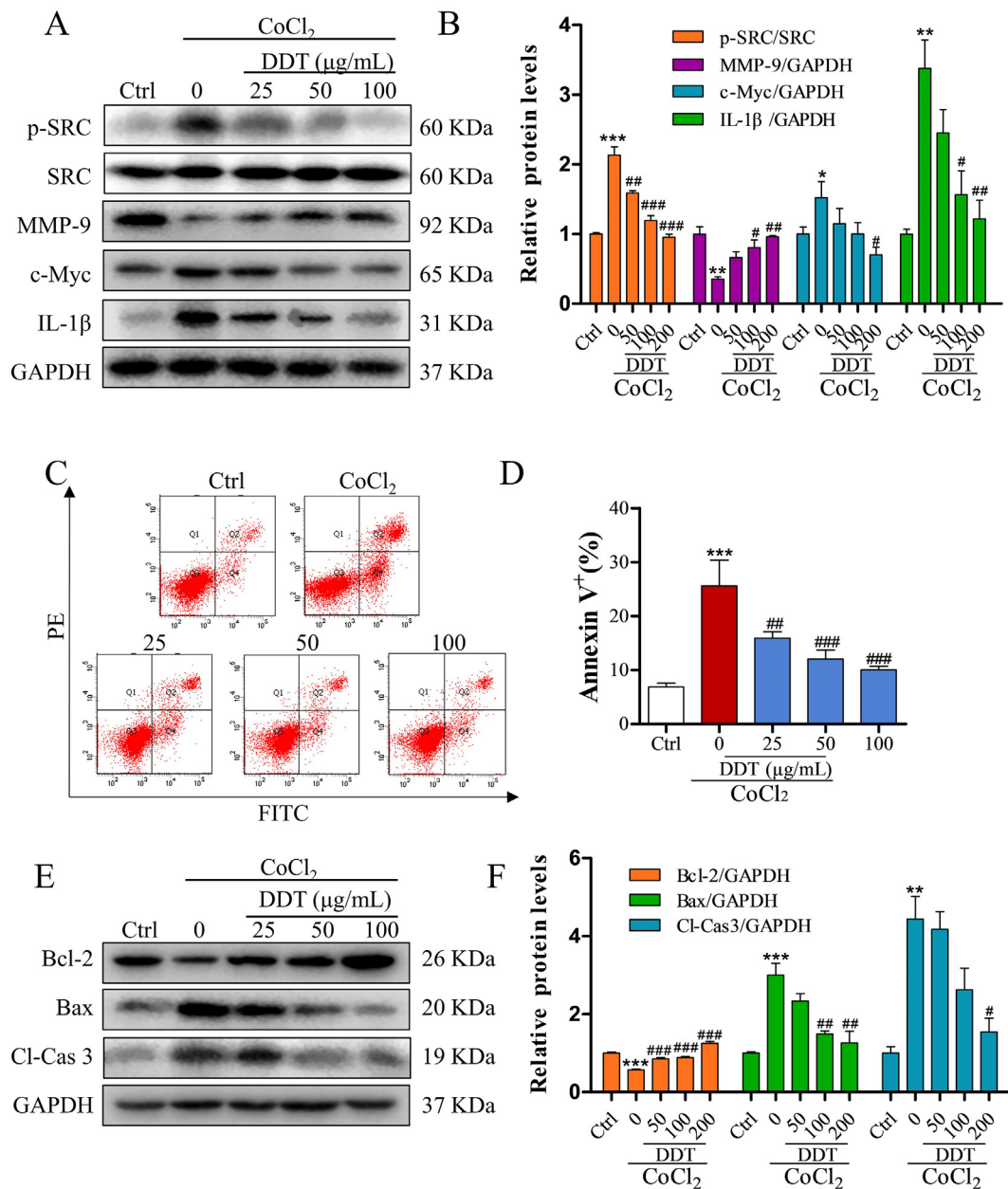
Figure 8. DDT protected against CoCl$_2$-induced PC12 cells apoptosis. (A) Western Blotting analysis of p-Src (Sup F. 19), Src (Sup F. 20), MMP-9 (Sup F. 21), c-Myc (Sup F. 22), IL-1β (Sup F. 23) and GAPDH (Sup F. 24). (B) Expression ration of p-Src, Src, MMP-9, c-Myc and IL-1β. (C, D) Typical histogram of apoptosis ratio was determined by flow cytometry. (E) Western blotting of Bcl-2 (Sup F. 25), Bax (Sup F. 26) and cleaved-Caspase 3 (Sup F. 27) with GADPH (Sup F. 28) as the internal control. (F) Quantitative analysis of the protein production levels. $*p < 0.05$, $**p < 0.01$, $***p < 0.001$ vs. Ctrl group; $^{#}p < 0.05$, $^{##}p < 0.01$, $^{###}p < 0.001$ vs. CoCl$_2$ model group.

may exert a neuroprotective effect by reducing apoptosis via ASK1/MKK7/JNK signaling pathway.

Our network pharmacological analysis found that the core proteins enriched of DDT treatment in ICH were most closely related to apoptosis and inflammation. DDT is composed of rhubarbs, peach seeds, leeches and gadflies. It has been reported that rhubarb has anti-an inflammatory effect, which may relate to aloe emodin, emodin and other substances [46, 47]. Aloe emodin and emodin belong to anthraquinone compounds, which have stronger hydrophobic effects, and resulting in a greater anti-inflammatory activity [48, 49]. Moreover, the anti-inflammatory and antioxidant activities of peach seeds are mainly due to their richness in phenols [50, 51]. For example, flavonoids, an important class of natural polyphenols, play important roles in inhibiting neuro-inflammation, repairing the blood-brain barrier, and inhibiting brain

damage [52, 53]. Leeches, as the most potent natural thrombin inhibitor, can inhibit oxidative damage and apoptosis induced by tissue ischemia [54, 55]. Research showed that hirudin can reduce the accumulation of leukocytes in the brain and shift microglia to the anti-inflammatory phenotype [56]. Therefore, hirudin plays a vital role in repairing the loss of neurons in the cerebral cortex. The main components of gadfly include fatty acids, ribonucleosides, pyrimidines, glycerol and derivatives. These components have been reported to modulate microglial polarization or inhibit lipid peroxidation levels from suppressing cellular inflammatory responses and apoptosis, stabilizing the balance of microvascular integrity, and reducing secondary brain injury [57, 58]. In summary, the anthraquinones, flavonoids, amino acids, unsaturated fatty acids and other compounds contained in DDT may be medicinal substances that exert anti-apoptotic and anti-inflammatory effects. Our
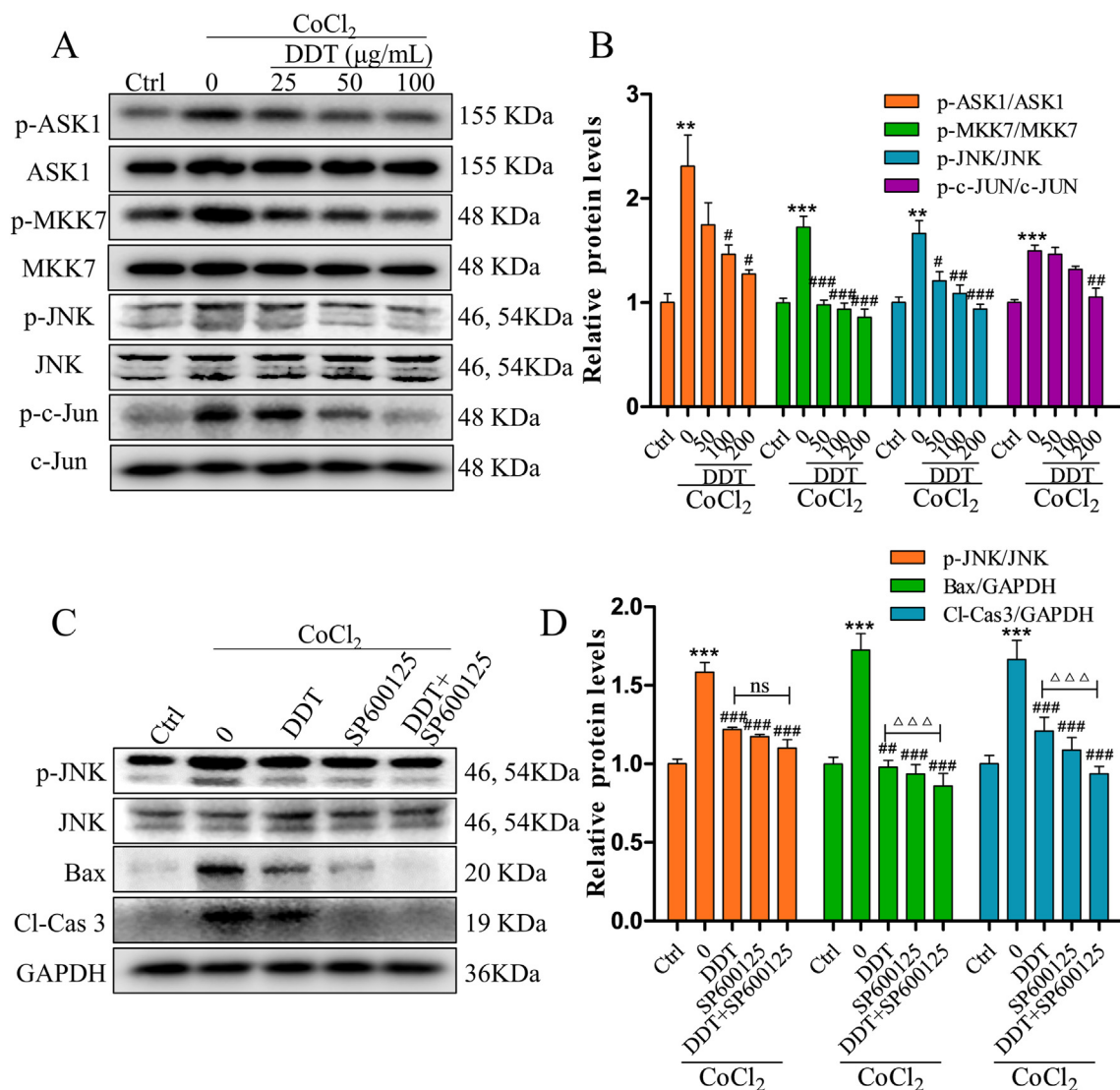
Figure 9. DDT ameliorated CoCl$_2$-induced PC12 cells apoptosis via ASK1/MKK7/JNK signaling pathway. (A) The expression of JNK signaling-related proteins p-ASK1 (Sup F. 29), ASK1 (Sup F. 30), p-MKK7 (Sup F. 31), MKK7 (Sup F. 32), p-JNK (Sup F. 33), JNK (Sup F. 34), p-c-JUN (Sup F. 35), c-JUN (Sup F. 36) by Western blot analysis. (B) Quantitative analysis of the protein production levels of (A). (C) PC12 cells were pretreated with the JNK inhibitor, SP600125 (20 μM) for 1 h, followed by exposure to CoCl$_2$, and/or DDT for 12 h. p-JNK (Sup F. 37), JNK (Sup F. 38), Bax (Sup F. 39) and cleaved-Caspase 3 (Sup F. 40) were evaluated by Western blot analysis with GADPH (Sup F. 41) as the internal control. (D) Densitometric results for Western blot are resented in the right panels. **$p < 0.01$, ***$p < 0.001$ vs. Ctrl group; #$p < 0.05$, ##$p < 0.01$, ###$p < 0.001$ vs. CoCl$_2$ model group. $^{\triangle\triangle\triangle}p < 0.001$ vs. DDT group.

interaction network analysis showed the intrinsic relationships between corresponding compounds of DDT and ICH (Figure 2B), in which emodin, aloe emodin, beta-sitosterol, succinic acid, hirudin, DLA, L-histidine may be the core ingredients.

5. Conclusion

To sum up the above, network pharmacology revealed the potential mechanism of DDT in the treatment of ICH. We identified 124 related targets, from which 6 nodes (including IL-1β, JUN, SRC, CASP3, MMP-9 and c-Myc) and two signaling pathways (MAPK and Apoptosis pathway) were elected as our central targets through topological feature analysis integrated with enrichment results. These enriched targets focused our attention on apoptosis. Subsequently, experimental validation in vitro and in vivo supplied convincing evidence that DDT exerted a neuro-protective effect by regulating ASK1/MKK7/JNK to inhibit neuronal apoptosis. Ultimately, our study will further demonstrate the efficacy and mechanism of action of DDT to guide its development as an effective treatment for ICH.

Data availability statement

Data included in article/supp. material/referenced in article.

Declaration of interest's statement

The authors declare no conflict of interest.

Additional information

Supplementary content related to this article has been published online at https://doi.org/10.1016/j.heliyon.2022.e11407.

References

[1] J.D. Burns, J.L. Fisher, A.M. Cervantes-Arslanian, Recent advances in the acute management of intracerebral hemorrhage, Neurosurg. Clin. 29 (2) (2018) 263–272.

[2] J.C. Hemphill 3rd, S.M. Greenberg, C.S. Anderson, K. Becker, B.R. Bendok, M. Cushman, G.L. Fung, J.N. Goldstein, R.L. Macdonald, P.H. Mitchell, P.A. Scott, M.H. Selim, D. Woo, C. American heart association stroke, C. Council on, N. Stroke, C. Council on Clinical, Guidelines for the Management of Spontaneous Intracerebral Hemorrhage, A guideline for healthcare professionals from the american heart association/american stroke association, Stroke 46 (7) (2015) 2032–2060.

[3] S. Chen, J. Peng, P. Sherchan, Y. Ma, S. Xiang, F. Yan, H. Zhao, Y. Jiang, N. Wang, J.H. Zhang, H. Zhang, TREM2 activation attenuates neuroinflammation and neuronal apoptosis via PI3K/Akt pathway after intracerebral hemorrhage in mice, J. Neuroinflammation 17 (1) (2020) 168.

[4] H. Lu, X. Ning, Y. Tao, J. Ren, X. Song, W. Tao, L. Zhu, L. Han, T. Tao, J. Yang, MEKK1 associated with neuronal apoptosis following intracerebral hemorrhage, Neurochem. Res. 41 (12) (2016) 3308–3321.

[5] E.K. Kim, E.J. Choi, Compromised MAPK signaling in human diseases: an update, Arch. Toxicol. 89 (6) (2015) 867–882.

[6] S. Chen, Y. Zuo, L. Huang, P. Sherchan, J. Zhang, Z. Yu, J. Peng, J. Zhang, L. Zhao, D. Doycheva, F. Liu, J.H. Zhang, Y. Xia, J. Tang, The MC4 receptor agonist RO27-3225 inhibits NLRP1-dependent neuronal pyroptosis via the ASK1/JNK/p38 MAPK pathway in a mouse model of intracerebral haemorrhage, Br. J. Pharmacol. 176 (9) (2019) 1341–1356.

[7] G. Samak, K.K. Chaudhry, R. Gangwar, D. Narayanan, J.H. Jaggar, R. Rao, Calcium/Ask1/MKK7/JNK2/c-Src signalling cascade mediates disruption of intestinal epithelial cell tight junctions by dextran sulfate sodium, Biochem. J. 465 (3) (2015) 503–515.

[8] Z. Huang, Y. Xia, K. Hu, S. Zeng, L. Wu, S. Liu, C. Zhi, M. Lai, D. Chen, L. Xie, Z. Yuan, Histone deacetylase 6 promotes growth of glioblastoma through the MKK7/JNK/c-Jun signaling pathway, J. Neurochem. 152 (2) (2020) 221–234.

[9] Y. Duan, S. Cheng, L. Jia, Z. Zhang, L. Chen, PDRPS7 protects cardiac cells from hypoxia/reoxygenation injury through inactivation of JNKs, FEBS Open Bio 10 (4) (2020) 593–606.

[10] L. Zeng, G. Tang, J. Wang, J. Zhong, Z. Xia, J. Li, G. Chen, Y. Zhang, S. Luo, G. Huang, Q. Zhao, Y. Wan, C. Chen, K. Zhu, H. Qiao, J. Wang, T. Huang, X. Liu, Q. Zhang, R. Lin, H. Li, B. Gong, X. Chen, Y. Zhou, Z. Wen, J. Guo, Safety and efficacy of herbal medicine for acute intracerebral hemorrhage (CRRICH): a multicentre randomised controlled trial, BMJ Open 9 (5) (2019), e024932.

[11] Z. Guo, S. Shi, W. Yang, M. Li, F. Zhang, The effect of zhu yu hua tan tang on intracranial pressure in case of acute cerebral hemorrhage, J. Tradit. Chin. Med. 20 (1) (2000) 3–9.

[12] Z.Y. Xia, J. Wang, J.W. Guo, R. Zhang, J.X. Li, J.B. Zhong, S.H. Luo, G.S. Chen, G. Huang, Q.S. Zhao, [Effect of Chinese drugs for breaking blood expelling stasis on acute cerebral hemorrhage: a prospective randomized double-blind controlled study], Zhongguo Zhong Xi Yi Jie He Za Zhi 36 (7) (2016) 821–826.

[13] Y. Lin, Study on application of the principle of eliminating stasis and refreshing spirit for acute stage of hemorrhagic apoplexy, J. Tradit. Chin. Med. 14 (2) (1994) 92–97.

[14] K.J. Chen, Blood stasis syndrome and its treatment with activating blood circulation to remove blood stasis therapy, Chin. J. Integr. Med. 18 (12) (2012) 891–896.

[15] S. Xu, Q. Pang, Z. Lin, N. Zhang, Effect of integrated traditional Chinese and Western medicine therapy for acute hypertensive intracerebral hemorrhage: a meta-analysis, Artif. Cell Nanomed. Biotechnol. 45 (6) (2017) 1–6.

[16] C.X. Danhui Yuan, Hong Lu, Qinglin Guo, Wenying Hu, Observation of curative effect on acute cerebral hemorrhage treated with didang tang and wuling san, J. Emerg. Tradit. Chin. Med. 14 (2005) 112–113.

[17] G.Z. Yan Sun, Observation on curative effect of didang decoction in treating 40 cases of cerebral hemorrhage, J. Zhejiang Coege of TCM 21 (1997) 38.

[18] J. Ren, X. Zhou, J. Wang, J. Zhao, P. Zhang, Poxue Huayu and Tianjing Busui Decoction for cerebral hemorrhage (Upregulation of neurotrophic factor expression): upregulation of neurotrophic factor expression, Neural Regen. Res 8 (22) (2013) 2039–2049.

[19] D.Z. Huiyu Dan, Jing Lu, Jian Wang, Effect of didang decoction on the expression of eIF2α, p-eIF2α and CHOP protein in rats with intracerebral hemorrhage, Jilin J. Chinese Med. 40 (2020) 792–795.

[20] J. Lu, Q. Huang, D. Zhang, T. Lan, Y. Zhang, X. Tang, P. Xu, D. Zhao, D. Cong, D. Zhao, L. Sun, X. Li, J. Wang, The protective effect of DiDang tang against AlCl3-induced oxidative stress and apoptosis in PC12 cells through the activation of SIRT1-mediated akt/nrf2/HO-1 pathway, Front. Pharmacol. 11 (2020) 466.

[21] Q. Huang, T. Lan, J. Lu, H. Zhang, D. Zhang, T. Lou, P. Xu, J. Ren, D. Zhao, L. Sun, X. Li, J. Wang, DiDang tang inhibits endoplasmic reticulum stress-mediated apoptosis induced by oxygen glucose deprivation and intracerebral hemorrhage through blockade of the GRP78-IRE1/PERK pathways, Front. Pharmacol. 9 (2018) 1423.

[22] A.N. Carey, D.R. Fisher, D.F. Bielinski, D.S. Cahoon, B. Shukitt-Hale, Walnut-associated fatty acids inhibit LPS-induced activation of BV-2 microglia, Inflammation 43 (1) (2020) 241–250.

[23] S. Mitra, J. Anjum, M. Muni, R. Das, A. Rauf, F. Islam, T. Bin Emran, P. Semwal, H.A. Hemeg, F.A. Alhumaydhi, P. Wilairatana, Exploring the journey of emodin as a potential neuroprotective agent: novel therapeutic insights with molecular mechanism of action, Biomed. Pharmacother. 149 (2022), 112877.

[24] Z. Ding, H.H. Da, A. Osama, J. Xi, Y. Hou, J. Fang, Emodin ameliorates antioxidant capacity and exerts neuroprotective effect via PKM2-mediated Nrf2 transactivation, Food Chem. Toxicol. 160 (2022), 112790.

[25] R. Li, W. Liu, L. Ou, F. Gao, M. Li, L. Wang, P. Wei, F. Miao, Emodin alleviates hydrogen peroxide-induced inflammation and oxidative stress via mitochondrial dysfunction by inhibiting the PI3K/mTOR/GSK3beta pathway in neuroblastoma SH-SY5Y cells, BioMed Res. Int. 2020 (2020), 1562915.

[26] Y. Bian, Y. Zhang, Z.B. Tian, Effect of hirudin on serum matrix metalloproteinase-9 of acute cerebral infarction: a protocol of systematic review and meta-analysis, Medicine (Baltim.) 99 (27) (2020), e20533.

[27] R. Zhang, X. Zhu, H. Bai, K. Ning, Network pharmacology databases for traditional Chinese medicine: review and assessment, Front. Pharmacol. 10 (2019) 123.

[28] S. Li, Network pharmacology evaluation method guidance-draft, World J. Trad. Chinese Med. 7 (1) (2021) 165–166.

[29] K. Kim, H.W. Park, H.E. Moon, J.W. Kim, S. Bae, J.W. Chang, W. Oh, Y.S. Yang, S.H. Paek, The effect of human umbilical cord blood-derived mesenchymal stem cells in a collagenase-induced intracerebral hemorrhage rat model, Exp Neurobiol 24 (2) (2015) 146–155.

[30] C.X. Shi, J. Jin, X.Q. Wang, T. Song, G.H. Li, K.Z. Li, J.H. Ma, Sevoflurane attenuates brain damage through inhibiting autophagy and apoptosis in cerebral ischemiareperfusion rats, Mol. Med. Rep. 21 (1) (2020) 123–130.

[31] R. Dogan, A.P. Sjostrand, A. Yenigun, E. Karatas, A. Kocyigit, O. Ozturan, Influence of Ginkgo Biloba extract (EGb 761) on expression of IL-1 Beta, IL-6, TNF-alfa, HSP-70, HSF-1 and COX-2 after noise exposure in the rat cochlea, Auris Nasus Larynx 45 (4) (2018) 680–685.

[32] Z. Zhang, L. Zhai, J. Lu, S. Sun, D. Wang, D. Zhao, L. Sun, W. Zhao, X. Li, Y. Chen, Shen-Hong-Tong-Luo, Formula attenuates macrophage inflammation and lipid accumulation through the activation of the PPAR-gamma/LXR-alpha/ABCA1 pathway, Oxid. Med. Cell. Longev. 2020 (2020), 3426925.

[33] Q. Huang, T. Lou, M. Wang, L. Xue, J. Lu, H. Zhang, Z. Zhang, H. Wang, C. Jing, D. Zhao, L. Sun, X. Li, Compound K inhibits autophagy-mediated apoptosis induced by oxygen and glucose deprivation/reperfusion via regulating AMPK-mTOR pathway in neurons, Life Sci 254 (2020), 117793.

[34] D. Zhang, Q. Cao, L. Jing, X. Zhao, H. Ma, Establishment of a hypobaric hypoxia-induced cell injury model in PC12 cells, Zhejiang Da Xue Xue Bao Yi Xue Ban 50 (5) (2021) 614–620.

[35] S. Yi, W. Shi, M. Zuo, S. Wang, R. Ma, H. Bi, B. Cong, Y. Li, Endoplasmic reticulum stress is involved in glucocorticoid-induced apoptosis in PC12 cells, Anal. Cell Pathol. 2021 (2021), 5565671.

[36] M. Grossetete, G.A. Rosenberg, Matrix metalloproteinase inhibition facilitates cell death in intracerebral hemorrhage in mouse, J. Cerebr. Blood Flow Metabol. 28 (4) (2008) 752–763.

[37] Z. Yuan, S. Gong, J. Luo, Z. Zheng, B. Song, S. Ma, J. Guo, C. Hu, G. Thiel, C. Vinson, C.D. Hu, Y. Wang, M. Li, Opposing roles for ATF2 and c-Fos in c-Jun-mediated neuronal apoptosis, Mol. Cell Biol. 29 (9) (2009) 2431–2442.

[38] H. Wang, P. Teriete, A. Hu, D. Raveendra-Panickar, K. Pendelton, J.S. Lazo, J. Eiseman, T. Holien, K. Misund, G. Oliynyk, M. Arsenian-Henriksson, N.D. Cosford, A. Sundan, E.V. Prochownik, Direct inhibition of c-Myc-Max heterodimers by celastrol and celastrol-inspired triterpenoids, Oncotarget 6 (32) (2015) 32380–32395.

[39] M. Morii, S. Kubota, T. Honda, R. Yuki, T. Morinaga, T. Kuga, T. Tomonaga, N. Yamaguchi, N. Yamaguchi, Src acts as an effector for ku70-dependent suppression of apoptosis through phosphorylation of Ku70 at tyr-530, J. Biol. Chem. 292 (5) (2017) 1648–1665.

[40] A.S. Mendiola, A.E. Cardona, The IL-1beta phenomena in neuroinflammatory diseases, J. Neural. Transm. 125 (5) (2018) 781–795.

[41] M. Cargnello, P.P. Roux, Activation and function of the MAPKs and their substrates, the MAPK-activated protein kinases, Microbiol. Mol. Biol. Rev. 75 (1) (2011) 50–83.

[42] J. Yue, J.M. Lopez, Understanding MAPK signaling pathways in apoptosis, Int. J. Mol. Sci. 21 (7) (2020).

[43] S. Li, C. Cong, Y. Liu, X. Liu, H. Liu, L. Zhao, X. Gao, W. Gui, L. Xu, Tiao Geng decoction inhibits tributyltin chloride-induced GT1-7 neuronal apoptosis through ASK1/MKK7/JNK signaling pathway, J. Ethnopharmacol. 269 (2021), 113669.

[44] A. Ju, Y.C. Cho, B.R. Kim, S.G. Park, J.H. Kim, K. Kim, J. Lee, B.C. Park, S. Cho, Scaffold role of DUSP22 in ASK1-MKK7-JNK signaling pathway, PLoS One 11 (10) (2016), e0164259.

[45] L.J. Li, J.C. Zheng, R. Kang, J.Q. Yan, Targeting Trim69 alleviates high fat diet (HFD)-induced hippocampal injury in mice by inhibiting apoptosis and inflammation through ASK1 inactivation, Biochem. Biophys. Res. Commun. 515 (4) (2019) 658–664.

[46] H. Gao, Y. Ren, C. Liu, Aloe-emodin suppresses oxidative stress and inflammation via a PI3K-dependent mechanism in a murine model of sepsis, Evid Based Complement Alternat Med 2022 (2022), 9697887.

[47] B. Hu, H. Zhang, X. Meng, F. Wang, P. Wang, Aloe-emodin from rhubarb (Rheum rhabarbarum) inhibits lipopolysaccharide-induced inflammatory responses in RAW264.7 macrophages, J. Ethnopharmacol. 153 (3) (2014) 846–853.

[48] X. Shang, L. Dai, J. He, X. Yang, Y. Wang, B. Li, J. Zhang, H. Pan, I. Gulnaz, A high-value-added application of the stems of Rheum palmatum L. as a healthy food: the nutritional value, chemical composition, and anti-inflammatory and antioxidant activities, Food Funct 13 (9) (2022) 4901–4913.

[49] D. Xin, H. Li, S. Zhou, H. Zhong, W. Pu, Effects of anthraquinones on immune responses and inflammatory diseases, Molecules 27 (12) (2022).

[50] X. Zhang, M. Su, J. Du, H. Zhou, X. Li, X. Li, Z. Ye, Comparison of phytochemical differences of the pulp of different peach [Prunus persica (L.) Batsch] cultivars with alpha-glucosidase inhibitory activity variations in China using UPLC-Q-TOF/MS, Molecules 24 (10) (2019).

[51] K. Foss, K.E. Przybylowicz, T. Sawicki, Antioxidant activity and profile of phenolic compounds in selected herbal plants, Plant Foods Hum. Nutr. 77 (3) (2022) 383–389.

[52] A.M. Alex Hamsalakshmi, M. Arehally Marappa, S. Joghee, S.B. Chidambaram, Therapeutic benefits of flavonoids against neuroinflammation: a systematic review, Inflammopharmacology 30 (1) (2022) 111–136.

[53] E. Tahanian, L.A. Sanchez, T.C. Shiao, R. Roy, B. Annabi, Flavonoids targeting of IkappaB phosphorylation abrogates carcinogen-induced MMP-9 and COX-2 expression in human brain endothelial cells, Drug Des. Dev. Ther. 5 (2011) 299–309.

[54] F. Davoodi, S. Taheri, A. Raisi, A. Rajabzadeh, A. Zakian, M.H. Hablolvarid, H. Ahmadvand, Leech therapy (Hirudo medicinalis) attenuates testicular damages induced by testicular ischemia/reperfusion in an animal model, BMC Vet. Res. 17 (1) (2021) 256.

[55] M.S. Sadati, M. Rezaee, S. Ghafarpur, F.S. Aslani, L. Dastgheib, R. Jahankhah, Cutaneous lymphoid hyperplasia induced by Hirudo medicinalis (leeches), J. Compl. Integr. Med. 16 (4) (2019).

[56] X. Li, Z. Zhu, S. Gao, L. Zhang, X. Cheng, S. Li, M. Li, Inhibition of fibrin formation reduces neuroinflammation and improves long-term outcome after intracerebral hemorrhage, Int. Immunopharm. 72 (2019) 473–478.

[57] M. Gu, Y. Li, H. Tang, C. Zhang, W. Li, Y. Zhang, Y. Li, Y. Zhao, C. Song, Endogenous omega (n)-3 fatty acids in fat-1 mice attenuated depression-like behavior, imbalance between microglial M1 and M2 phenotypes, and dysfunction of neurotrophins induced by lipopolysaccharide administration, Nutrients 10 (10) (2018).

[58] X. Chen, C. Chen, S. Fan, S. Wu, F. Yang, Z. Fang, H. Fu, Y. Li, Omega-3 polyunsaturated fatty acid attenuates the inflammatory response by modulating microglia polarization through SIRT1-mediated deacetylation of the HMGB1/NF-kappaB pathway following experimental traumatic brain injury, J. Neuroinflammation 15 (1) (2018) 116.